THE ‚ERAY' AIRCRAFT CONCEPT

A. Frühbeis, I. Held, P. Sieb, A. Usbek, Technische Universität München, München

Abstract

The eRay conceptual design meets the future demand for ultra efficient aircraft. A qualitative study examines various basic concepts and defines the framework of a turbo-electric distributed propulsion (TEDP) aircraft with Laminar-Flow Control for improved aerodynamics and CFRP structures for decreased mass. The TEDP layout is further specified to consist of electric fans distributed along the wing and around the aft fuselage. The electric engines are powered by a turbine and a generator placed on each wing tip and a battery for buffering. A parametric model links aerodynamics, mass estimation and propulsion creating a simulated model of the reference airplane and the investigated concept. Iterating over several input parameters led to a conservative and a more optimistic concept to consider uncertainties regarding technical and social developments until 2045. The technical concepts differ through qualitative input parameters like battery energy density and through bolder design features like the lack of a vertical stabilizer. The optimistic version leads to the promoted concept eRay, showing mass reductions of 30%, (L/D) improvement of 24% and propulsive efficiency improvements of 50% compared to 2005's state-of-the art reference aircraft leading to an overall improvement in energy consumption of 64% compared to the Airbus A321. The 'Baseline Concept' is 47% more efficient regarding energy consumption than the selected reference airplane. Ground handling of the aircraft requires certain minor adjustments in airport technical infrastructure. However, the concept of operations and considerations regarding cabin layout and the technical and financial feasibility show the competitiveness of the eRay in an airline's daily routine, proofing that the eRay meets the demands specified in the beginning.

1. INTRODUCTION AND MARKET ANALYSIS – ROADMAP 2045

The amount of global revenue passenger kilometers (RPKs) has been growing on average by 5.5% in the last decade [1]. Energy production has become more lavish and resource-consuming as well as more incisive to nature. Oil and gas are produced by fracking or the ongoing exploitation of lignite [2]. This growth rate will only receive global and social acceptance if it can be achieved with a decreasing environmental footprint. Reducing the air transport's energy share and meeting the ambitious goals set by the European Commission in Flightpath 2050 and NASA, new aircraft designs are inevitable [3, 4]. At the same time, social change will also impel the demand of future aircraft configurations. By 2045, the world population has exceeded 9 billion humans and more than 60% of that population lives in urban areas [5]. The above-average population growth around Asian cities combined with a fast-rising middle class will boost the demand for air travel capacities in the Asia-Pacific region [6]. Today, 14 of the 20 most frequently served routes are short haul flights connecting Asian cities [7].

This market promises high economic potentials for aircraft manufacturers and airlines in the next decades and is the key market to our concept [8]. Besides, energy consumption and associated pollutants combined with noise emissions of aircraft are very critical for on-ground handling, take-off and landing. Aircraft noise has been held responsible for sicknesses of residents [9]. Several hubs like Amsterdam, Zurich and Stockholm have introduced noise charges and others will follow [10, 11, 12]. Extensions at airports such as London Heathrow or Munich Airport have been planned for decades, however it is questionable if they will ever be realized [13, 14]. Hence, airport capacity in North America's and Europe's big airports will remain the same or just see a very slight increase and therefore become a bottleneck for air transport growth. By 2050, the demand for almost 4 million flights in Europe might not be satisfied due to airport capacity constraints [15]. Not only the attitude of residents living close to airports has become more discerning, also the wishes of passengers have undergone a change. Almost 60% of all passengers bypass their local airport and drive further accessing a direct flight [16]. The daily nonstop coast-to-coast services in the United States have more than doubled in the last 20 years [17], in Europe the number of direct flights has grown by more than 110% between 2003 and 2013, whilst the overall commercial aircraft fleet has only increased by 25% [18]. Future aircraft concepts have to satisfy the trend for more point-to-point connections, linking smaller airports directly with each other. The addressed challenges of the previous section form the following requirements for the aircraft concept:

- Saving energy of 60% and more
- Feasibility of flying over water for at least 3h
- Point-to-point connection between smaller airports
- Low noise and emissions enabling the extension of airport operating hours
- Affordable manufacturability
- Reducing operating costs

2. METHODOLOGY

As a reference, the airplane A321-200 WV011 [19] with 93.5t Maximum Take-off Weight (MTOW) is selected. The first selection of airplane layouts is made by qualitative means. Afterwards, a quantitative evaluation is made based on an iterative parametric model. This model implements empirical and quasi-analytical formulas known from literature and is calibrated against the A321. For the final concept, parameter studies are conducted to optimize

doi:10.25967/480345

performance. Additionally, the calculation is refined using CAD models for zero-drag calculation and structural analysis. Finally, there are three models developed: the A321, a baseline concept and an optimistic concept which can be compared by means of mass, aerodynamics and energy efficiency. These two different concepts are based on scenario analysis. Some future trends like the development of the global population can be forecasted with only little uncertainty, but others like the development and acceptance of new technologies or a change of admission regulations do not allow an equally precise estimation over a time period of 25 years. The baseline scenario represents conservative extrapolation, whereas the best-case scenario is more optimistic about technology development, societies' openness towards innovations and minor adaptions of the admission regulations.

3. CONCEPT SELECTION

As requirements are set, different approaches to meet these are evaluated. In addition to structure, major technical topics are aerodynamic efficiency and overall efficiency of the propulsion system with the performance indicators glide ratio (L/D) and overall efficiency η_{ov}. Here, η_{ov} is defined as the product of propulsive efficiency of the fans, electric efficiency of all electric components and core efficiency of the gas turbine.

3.1. Basic Design Consideration

For increasing propulsive efficiency, open-rotor systems, geared turbofans, electric propulsion and turbo-electric propulsion (TEDP) are investigated. All four approaches increase the accelerated mass flow, decrease exit velocity and thus increase η_{prop} (see section 4.3.1). This is done, except for the "all electric" airplane, by increasing the Bypass-Ratio (BPR). The decision for one of these concepts is made on a qualitative basis using a decision table (see BILD 13 Appendix). This takes among others into account weight, efficiency, noise and potential synergy effects.

Open-rotor suffers from an efficiency drop with increasing Mach number, high noise and an increased risk in case of blade-off, especially in contrast to a geared turbofan. However, with this concept it is complicated to make use of synergy effects such as boundary layer ingestion (BLI), as this would affect the core efficiency. In contrast, (turbo-)electric propulsion allows greater design freedom and thus potentially more synergy effects, but at the cost of transmission losses and higher system complexity. For this concept, it is decided to continue with (T)EDP to investigate its synergy effects.

The aerodynamic layout evaluation is made on the assumption of implementing TEDP and new materials as CFRP. It is compared to the conventional fuselage of a A321 (see BILD 1). Points more outside represent better solutions. A significant improvement in aerodynamics can be achieved by reducing the viscous drag, either through drastically reducing the wetted area or by laminarization of the flow (LFC). The first approach is implemented effectively by all-wing or blended wing bodies (BWB). However, this type not only requires major changes in production and operation, but also passenger acceptance is critical due to multiple changes, e.g. stronger flight movements [25]. Furthermore, a BWB's adaptability for family concepts is low compared to conventional layouts. A compromise between conventional and BWB configuration is the double bubble fuselage, that also reduces wetted area per PAX, without significantly reducing passenger comfort. However, the potential for synergistical propulsion implementation and aerodynamic improvement is limited.

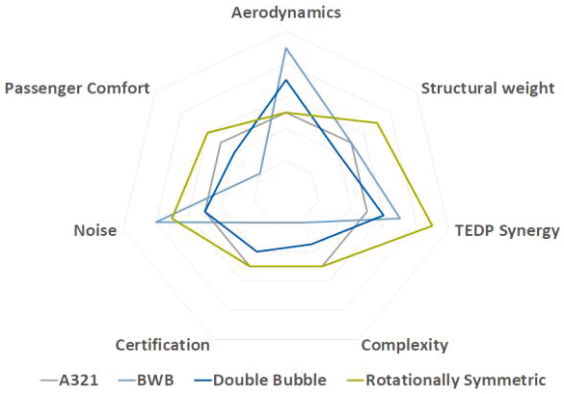

BILD 1 Layout under the assumption of implemented TEDP

According to the previously mentioned arguments, this concept sticks to the conventional fuselage-wing layout. For improved aerodynamics, laminarization of the flow around the wings is implemented.

3.2. Refined Layout

As the approaches to meet aerodynamic and propulsive efficiency are set, the layout has to be considered more closely. TEDP offers great design freedom which inherits several opportunities, but thus requires a well-structured approach to evaluate these, especially because of its interference with the aerodynamic layout. A selection of options can be seen in BILD 2. According to [26], the Propulsive Fuselage (PF) offers the greatest potential for power savings, as the influence of BLI (see section 4.3.1) is most significant at the aft of the fuselage. Consequently, this concept is selected for implementation. However, the PF performs best if used only for compensating the fuselage-drag, thus a secondary thrust-source is needed. One option is to remain at conventional aircraft configuration using two geared turbofan turbines, but as electric distributed propulsion, contrary to gas-turbines [27], does not have the disadvantage of dropping efficiency when scaled smaller, additional EFANs are also feasible.

Concept	Description and Abbreviation
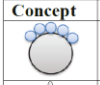	Aft-mounted fans covering the upper part of a cylindrical fuselage (REVOLVE)
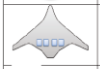	BWB with embedded fans on top of the lifting body trailing edge (BWB)
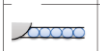	Tube and wing configuration with fans integrated within a split-wing (SPLIT)
	Tube and wing concept with fans mounted on the upper wing side (WING)
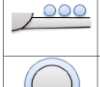	Cylindrical fuselage with circumferential fan at the aft section (PROPFUS)
	Cross-flow fan embedded into the trailing edge of the wing (CROSS)

BILD 2 Selection of possible TEDP layouts - Originating from Source [26]

Remaining configurations that are applicable are SPLIT, WING and CROSS (see BILD 2). All three offer the possibility of wake-filling of the wing, CROSS and WING additionally allow BLI. However, transmission efficiency of CROSS and its high relative Mach numbers are critical for transonic operating aircraftl. SPLIT does not allow BLI and its size is limited by the local wing geometry, but by implementing WING, increased interference drag with the wing is critical. Eventually, the WING configuration is chosen, as it allows a higher degree of design freedom. At a later stage of this report it is shown that pure electric propulsion would not be feasible, even if calculated with very optimistic energy densities in the year 2045 (see section 4.3.3), thus gas-turbines are implemented. The gas turbines are placed at the wing tips for load relief at the root, end-plate effect and undisturbed inlet-flow. As they are primarily used for power generation and only deliver 1.2 kN thrust each, One Engine Inoperative (OEI) is uncritical even if implemented at the wing tip.

4. THE CONCEPT: TECHNICAL SPECIFICATION

The approach presented in this paper was primarily to increase the propulsive efficiency using turbo-electric distributed propulsion (TEDP), to improve the aerodynamics using Laminar- Flow Control (LFC) and reduce weight by new materials, a new fuselage concept and active load reduction. After the evaluation of different possible implementations (see section 3), one concept is investigated in detail and two variants are derived. One variant is a low-risk concept, that is based on a baseline scenario where all certification-requirements of today are met, and technology has improved only incrementally, resulting in fuel-saving of 52% compared to 2005 for a mission with a distance of 4200km and maximum payload. Furthermore, a more optimistic concept eRay is derived, assuming changes in admission as well as changed requirements by passengers and disruptive improvements in key technologies e.g. battery capacity and cooling technologies, resulting in fuel savings of 65%.

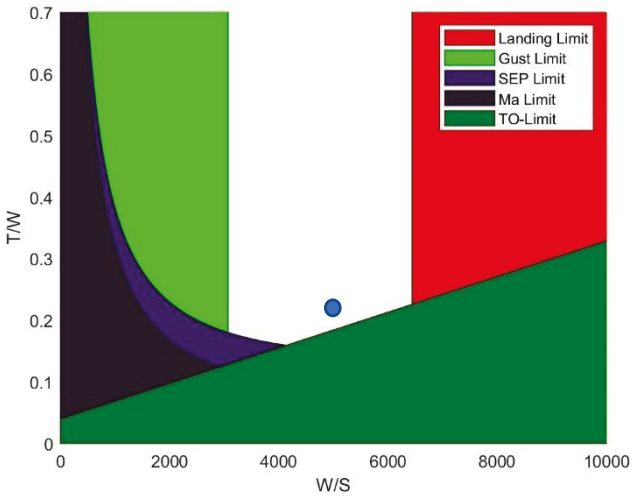

BILD 3 Design Chart of eRay

The optimistic model eRay has quite a small take-off mass of 67t and increased wing area, since the reduced viscous drag leads to a lower optimum C_L of 0.4 for cruise. Therefore, wing loading is relatively small with 4870 N/m², but as can be seen in BILD 3, still not critical for gusts. The static thrust delivered by EFANs and PF reaches 152kN, meeting the required Thrust-to-Weight ratio of 0.23. The wing area of 135m² as well as the sweep of only 22° is beneficial for high lift at take-off and landing. Additionally, the distributed EFANs on the aft of the wing are used for boundary layer control to avoid flow detachment at high angle of attack and externally blown flaps are implemented behind them (see BILD 4). Therefore, a complex high lift system is avoided.

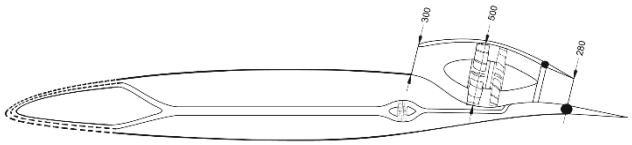

BILD 4 Cross Section of the wing

4.1. Structure and Masses

	A321	Baseline	Best
Max. TO Mass	93500	75500	67000
Empty Mass	49400	41600	35600
Propulsion total	7006	7696	5582
- Gas Turbines (Generators incl.)	7006	3201	2403
- EFANS	0	1710	939
- PF	0	952	634
- Converters	0	1831	815
- Refrigerator	0	0	789

TAB 1 Propulsion mass in kg

In Table 1 the maximum take-off mass decreased from 93.5t to 67.0t while reducing empty mass from 49.4t to 35.6t. In BILD 5, a breakdown of all main components of the A321 and the two investigated concepts can be seen. It is clearly visible, that kerosene mass is the major driver for reduced MTOW, as the eRay carries 15t less for a mission of 4200km. Payload in high density configuration is set to 25.2t, consisting of 21.2t for 212 passengers and 4t for freight. Structural components are made of carbon fiber and are additionally lighter due to less take-off weight. The mass of the fuselage is decreased by excluding windows. The wing benefits from the assembly of propulsion, as with gas-turbines and generators placed at wing tips, a reduction in wing root bending moment of 5.5% is achieved compared to a conventional placement. To counteract the moment of the PF at the aft fuselage, the battery is placed in the belly right before the wings for a center of gravity at neutral point. The neutral stable configuration is further explained in section 4.4. Moreover, the eRay features an active maneuver and gust load alleviation system. The flaps adapting the EFANs outlet cross section to flight conditions and the ailerons are used to reduce loads incorporated by gusts and maneuvers. The ultimate load factor for eRay is consequently reduced from 3.75 to 3.0.

As only a horizontal tail is installed in the eRay, the mass of the empennage is reduced (see section 4.4). System mass declines as the hydraulic system is replaced by electric actuators, no APU is necessary anymore, the high lift device is more simple and electric power generation and

storage is already included in the propulsion system and battery mass. The propulsion mass increases in the baseline concept from 7.0t to 7.7t due to higher system complexity because of electric motors, generators and converters additional to gas turbines. For eRay, this development is met by the use of superconducting electrical components, reducing propulsion weight to 5.6t. The refrigerator is estimated to increase weight by an additional 70% of the generator or motor that is supposed to be cooled by it [28]. Furthermore, batteries must be installed as buffer for high energy demand at takeoff and climb. Turbine weight decreases as an effect.

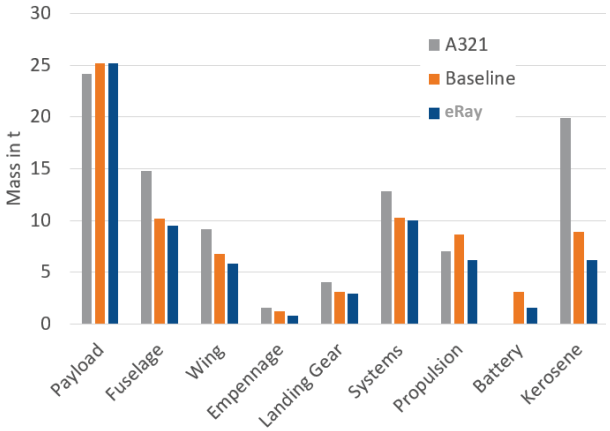

BILD 5 Mass of Aircraft Components

4.2. Aerodynamics

Key indicator in aerodynamics is the glide ratio C_L/C_D, consisting of the lift coefficient C_L and the drag coefficient C_D. The glide ratio of the A321 is calculated to be 17.3, while the eRay has a glide ratio of 22.1. This improvement of aerodynamic efficiency is mainly achieved by holding major parts of the wing's boundary layer laminar using the OA-JTI-1 airfoils and LFC, reducing wetted area with the empennage and optimizing induced drag. Firstly, C_L is determined by a trade-off between the wing's viscous and induced drag. The minimum is C_L = 0.4, where induced drag equals viscous drag. The wing's area of 135 m² is calculated using the force equilibrium in cruise. With a sweep angle of 22° determined in 4.2.1, the taper ratio λ is chosen for an almost elliptical lift distribution to 0.24 [21, 29]. As the next step, the Aspect Ratio (AR) is chosen. BILD 7 shows dependencies of wing mass (WM), wing span (WS) and energy consumption for eRay's fixed C_L. The trend of the energy consumption points out that an AR of 25 is favorable. However, ground handling and infrastructure is limiting, thus, the wingspan is set to 38m. This is a compromise between low energy consumption and still being capable of operating at airports with a limited box size of 36m. The difference of 2m is addressed by a highly maneuverable landing gear.

Viscous Drag: For a subsonic aircraft, the drag coefficient is the sum of zero drag and induced drag coefficient. Zero drag is calculated using parasite drag areas according to Torenbeek [20] as seen in BILD 6. The transition from laminar to turbulent occurs at 60% of the profile's chord for this concept, as shown in [30]. Together with a new empennage, $c_{d,0}$ is improved by 30%.

Induced Drag: The induced drag is calculated by $C_{ind} = k * c^2{}_L$, with $k = 1/(\pi * AR * e_{eff})$. Due to the end plate effect, the Oswald factor e_{eff} improves by 7.8% using following equation: $e_{eff} = (1 + 2 * h_{turbine}/b)^2 * e$ [31]. Compared with the A321, the eRay has higher AR, uses end plate effect and especially reduces C_L from 0.58 to 0.4, resulting in a reduction of induced drag of 56%.

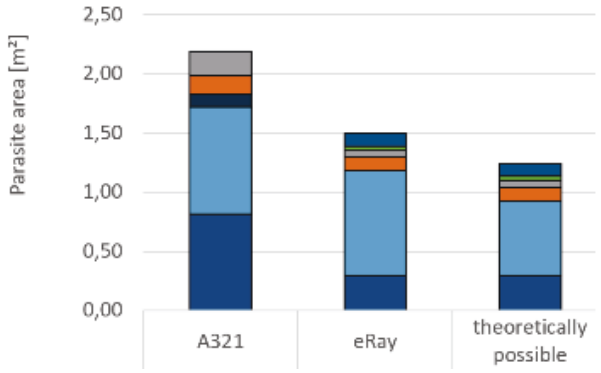

	A321	eRay	theoretically possible
Efans	0,00	0,11	0,11
Propfuse	0,00	0,04	0,04
Gasturbine	0,21	0,06	0,06
Horizontal-Tail	0,16	0,11	0,11
Vertical-Tail	0,11	0,00	0,00
Fuse	0,90	0,89	0,63
Wing	0,82	0,29	0,29

BILD 6 Parasite Areas

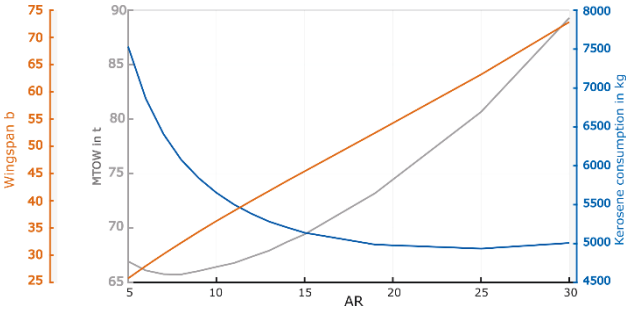

BILD 7 WS, MTOW and kerosene consumption over AR

4.2.1. Laminar Flow Control

Instability mechanisms as Tollmien-Schlichting instability (TSI), Cross-flow instabilities (CFI) and Attachment-line transition (ALT) lead to a transition from laminar to turbulent flow. Suction of air at the first 20% of wing chord can control sweep-induced crossflow disturbances of highly swept wings, that are usually required for flying at high subsonic and supersonic speeds. Hence, removing a small amount of the boundary layer air by suction through porous material is applied. Furthermore, suction at the leading edge can avoid ALT. As shown in flight and wind tunnel experiments, TSI predominates on aircraft wings with moderate leading-edge sweep angles Λ_{LE}< 25° [32]. With airfoil OA-JTI-1 the laminar bucket reaches a C_L of up to 0.5, providing eRay's wings with a tolerance before transition [30]. Using natural laminar airfoils, the shock and pressure recovery occurs at

a high chord length. Shock strengths are limited by a local Mach numbers of 1.2 to prevent shock-induced separation of the laminar boundary layer. To ensure attached flow, the maximum slope of the aft pressure gradient $\Delta c_p/\Delta(x/c)$ is kept below 3.0. The airfoil's Ma_{Design} is 0.724 [30]. As eRay cruises at Mach 0.78, the sweep angle is determined to 22° reducing the effective Mach number to 0.724. As the airfoil's design Mach number is calculated in [30] for a different Reynolds number and C_L, the Korn equation (eq. (1)) is used to determine if wave drag is still acceptable. With a thickness of 0.14, the Korn equation leads to a divergence Mach number of 0.725, that is very close to the design Mach number [33]. Thus, the chosen wing represents a good trade-off between high velocity and low wave drag.

$$(1)\quad \mathrm{Ma}_{dragdivergence} = \frac{K}{\cos(\Lambda_{LE})} - \frac{\frac{t}{c}}{\cos(\Lambda_{LE})^2} - \frac{c_{l,design}}{10\cos(\Lambda_{LE})^3} = 0.725$$

The airfoil technology factor K in eq. (1) is assumed to be 0.87 taken from data of the NACA 6 series [30]. t/c is the thickness-to-chord ratio. A pressure difference Δc_p of 0.2 is applied between the wing surface and the suction chamber [34]. The pressure difference of the wing can be calculated to 4.5 kPa. The suction speed u_s is defined as $c_Q * U_\infty$ where c_Q is the suction coefficient [35]. Integrating the suction coefficient over the chord and multiplying with U_∞ delivers the mean speed of 0.078 m/s. With that the suction mass flow over the whole wing can be calculated to 1.5 kg/s. Energy consumption can be calculated to 20 kW. As a result, a reduction of zero drag of the wing of 50% is achieved by the LFC for the eRay, leading to an overall better (L/D) of 26% due to LFC, which is in accordance with literature [36].

4.3. Propulsion

In both concepts, instead of producing thrust with conventional gas turbines, thrust is decoupled from the core engines. The core engines drive generators to produce electric energy. The turbines are placed at the wing tips, as in case of OEI only a limited yawing-moment results. The EFANs are placed on the trailing edge of the inner top wing (see BILD 16 Appendix), and thus enable better propulsive efficiency, enhanced Laminar-Flow-Control and super-circulation [37]. A spacing of 1.5m from the fuselage is provided to avoid interference with the PF. The PF is placed at 95% fuselage-length to take full advantage of BLI. Due to multiple redundancy by the PF and multiple EFANs, in case of OEI the yawing moment can be fully compensated by the remaining fans, resulting in a smaller vertical tail [29] for the Baseline. Additionally, the EFANs are responsible for yaw-control and thus replace the rudder. For the eRay, certification changes are assumed to enable neutral directional stability. Thus, the complete vertical tail and rudder is replaced by a horizontal tail with dihedral angle and by thrust variation of EFANs. Additionally, the drag of the fuselage is compensated by an electric turbine at the end of the fuselage (Propulsive Fuselage PF), further increasing propulsive efficiency. The EFANs have the disadvantage of increased wetted area due to the space in between them. This is counteracted by filling this space with the actuators of the flaps, replacing flap track fairings.

In contrast to the common approach, following advantages are implemented due to TEDP:

1) Electric engines can be scaled smaller without significant efficiency loss. Thus, they can be distributed without penalty. In this concept, electric fans are placed at the trailing edges of both wings and at the end of the fuselage (see BILD 16 Appendix).
2) EFANs are put into the boundary layer (BLI), thus improving η_{prop} by reduced ram-drag and wake-filling, without disadvantages in core efficiency [26]
3) A battery is used as a buffer for high power demands. Consequently, the core engine can be scaled smaller and is optimized for one design point. Additionally, NOx and carbon dioxid near populated areas during taxiing, take-off and landing are completely avoided using the required power from the battery.
4) In case of OEI of a gas turbine, thrust is still provided by EFANs and battery.
5) High redundancy, as 20 EFANs plus one PF are used.
6) Replacement of rudder and vertical tail in best case concept allows reduction in wetted area.
7) Due to the placement on the rear top of the wings, super-circulation is implemented, avoiding a complex and noisy high-lift device [38].

As a result, the overall efficiency of the propulsion system increases by 25% for the Baseline and by 50% for the eRay. The overall improvement consists of 29% more efficient gas turbines and an improvement in propulsive efficiency of 23%.

4.3.1. Propulsive Efficiency

Propulsive efficiency is defined as the ratio of thrust performance to usable power. For an adjusted nozzle, the ideal propulsive efficiency η_{prop} can be stated as:

$$(2)\qquad \eta_p = \frac{T\cdot V_\infty}{P} = \frac{\dot{m}(V_2 - V_1)\cdot V_\infty}{\frac{\dot{m}}{2}(V_2^2 - V_1^2)} = \frac{V_\infty}{V_1 + \frac{V_2 - V_1}{2}}.$$

Propulsive efficiency can either be improved by reducing specific thrust $V_2 - V_1$,or by BLI with the effect of decreased inlet velocity V_1 [39, 26]. The first approach leads through a higher BPR to increased massflow, reduced total pressure ratio PI and increased inlet area and nacelle drag. Thus, determining the optimum specific thrust is a trade-off between those. In BILD 8, the optimum for kerosene consumption can be determined by PI=1.15 or a specific thrust of 41 m/s respectively. The second approach leads to higher specific thrust, as V_1 is reduced. However, for the EFANs the effect is marginal, as the boundary layer is thin.

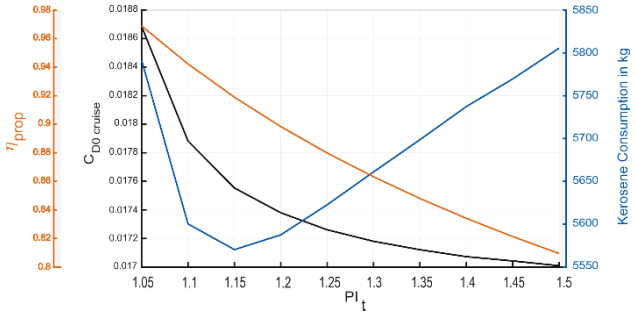

BILD 8 Propulsive efficiency, zero drag and kerosene consumption over total pressure ratio of EFAN

In contrast, the PF profits significantly from BLI, as boundary layer thickness at the aft fuselage is 0.46m. This value determines the inlet height according to [40]. For best performance, the thrust of the PF is set to compensate the impulse loss of the fuselage in cruise. With this propulsion system, the combined η_{prop} could be increased by 23% compared to the CFM56.

4.3.2. Optimizing Turbine Technology

To evaluate the most efficient engine technology, several concepts were compared in GasTurb12. The most promising is a core concept presented by EU funded research program LEMCOTEC using both, an intercooler in between the compressors as well as recuperation, called Intercooled Recuperated Aero Engine (IRA) and promising real PSFC savings of 20% compared to turbofan configurations. [39, 41, 42]. Unlike traditional engine designs, Power Specific Fuel Consumption (PSFC) does not improve with a higher Overall Pressure Ratio (OPR) but deteriorates slightly [39]. Even if the primary goal is reducing the energy consumed, NOx emissions are not completely neglected for the turbine's design. According to the Aeronautics and Space Engineering Board, NO_x emissions are a nonlinear function of P3 and T3 [43]. Hence, the IRA concept is beneficial to reduce fuel burn and NO_x emissions at the same time. In addition, the flight Mach number has almost no negative influence on the core efficiency [39]. Therefore, the intercooler and recuperator are integrated to eRay's turbines. Boosting combustion temperature is the most effective way of boosting the core efficiency. Today, turbines with a Turbine Entry Temperature (TET) of 1850 K are already in service e.g. the M88-2, engine of France's Rafale using ceramic coating on the turbine blades [39]. With a yearly improvement of 12K in TET over the last decades, the assumption of TET of approximately 1840K and a burner temperature of 1900K for eRay' turbines has two supporting reasons [39]. For the baseline scenario a less optimistic combustion temperature of 1800 K is assumed. BILD 14 in the Appendix shows the turbine's performance data at cruise (Mach 0.78, FL 330, ISA conditions). Results of a multi-parameter optimization in GasTurb12 show optimal PSFC for an OPR of approx. 25 in BILD 14 Appendix. However, the variation of PSFC within an OPR between 22 and 30 is less than 2 h. At the same time, a higher OPR of 30 promises NO_x savings of 2 %. To select an optimal Design Point (DP), PSCF is plotted against SP in BILD 14 Appendix (b): With an increasing PSFC the SP rises, meaning a conflict of interest between a low PSFC and a high SP. The SP increases by about ten times the percentual magnitude of the PSFC rise. Therefore, a slight deviation of around 2 ‰ from the optimal PSFC was chosen to be eRay's DP. That offers a higher SP and consequently smaller turbines inducing less aerodynamic drag as well as a better NO_x Emission Index. The OPR is 29.5 at DP; the DP is plotted in BILD 14 Appendix (b). The NO_x is slightly less than 0.65. However, new combustion technologies as the Rich-Quench- Lean and Lean Premixed Prevaporised combustion offer chances of significantly reducing NO_x emissions by up to 85% [39, 44].

The new combustion technologies are not modelled in GasTurb12 and therefore, NO_x are regarded as less critical since they can be significantly reduced. An overview of the engine's data at cruise for both scenarios can be found in Table 2. The core efficiency improves for the eRay by 29% compared to A321. Regarding the engine's operation, the startup process is also considerably slowed down compared to a regular turbofan. As a consequence, lower temperature gradients and transient centrifugal forces are applied on the engine. The constant TET and the slower start up process will contribute to a significant reduction of wear of high temperature parts like blades in the turbine and to less maintenance [45].

	Power [kW]	OPR [-]	T4 [K]	TET [K]	PSFC [kg/(kWh)]	η_{Core} [%]
eRay	3521	29.5	1900	1838	0.146	57.3
Base	5015	23.9	1800	1741	0.148	56.3

TAB 2 Single Engine data

4.3.3. Battery System

The batteries deliver energy during takeoff and for the first part of climb and also replace the auxiliary power unit (APU). Until 2010, battery density has improved by 7% p.a. [40]. Combined with lithium ion batteries featuring a capacity of 335 Wh/kg available in 2010, extrapolation suggests a density of more than 2500 Wh/kg by 2040 [46]. However, this assumption appears to be too optimistic, as there are lower theoretical limits for Li-ion batteries, and promising announcements could not be met and the last European technology group quit the market recently [47]. The theoretical limit for Li2S/Si batteries is 1550 Wh/kg, though the typical realistic battery density is approximately half of the theoretical limit [46]. Consequently, the baseline scenario assumes a conservative estimation of half of the theoretical limit: 800 Wh/kg. eRay features a higher density of 1400 Wh/kg, assuming a breakthrough in battery technology as Lithium- Sulfur and Lithium-Air combinations offer high potential densities [46, 48].

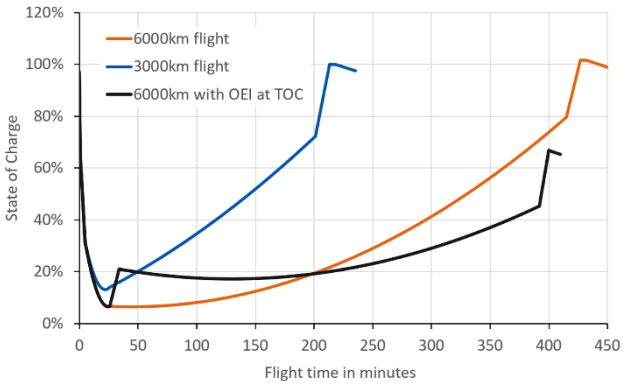

BILD 9 Battery Capacity during flight time

BILD 9 shows the state of battery charge during flight, the blue line is a flight of 3000km with the single class layout, the orange line representing the same aircraft configuration flying 6000km. During climb, the 6000km configuration is heavier and therefore needs more energy. Consequently, it has less remaining energy in the batteries as it reaches Top of Climb (TOC). During the longer cruise duration, the batteries can be charged slower than for a 3000km mission. With ongoing flight duration, the eRay gets lighter and less energy is required for propulsion as eRay climbs steadily. More excess power can be transferred to the batteries. The

remaining 20% to 25% are charged during descent, when eRay glides and uses the full energy delivered by the engines for charging. From 2000m altitude onward, the gas turbines are switched off and the last kilometers are powered by the batteries only. The black line shows a One Engine Inoperative (OEI) event for one turbine at the most critical point: TOC. The batteries are almost emptied and eRay descends to FL 165 immediately. Air speed is reduced to Mach 0.56 continuing operation at optimal C_D/C_L ratio and increasing engine's power. Under these conditions, the batteries deliver auxiliary energy until enough fuel is burnt and the minimum of the black curve is passed approx. 180 min after takeoff. From now on, the remaining engine provides enough power for propulsion and is even capable of charging the batteries. The black line displays that eRay will exceed the requirements for an Extended Operations of ETOPS 180.

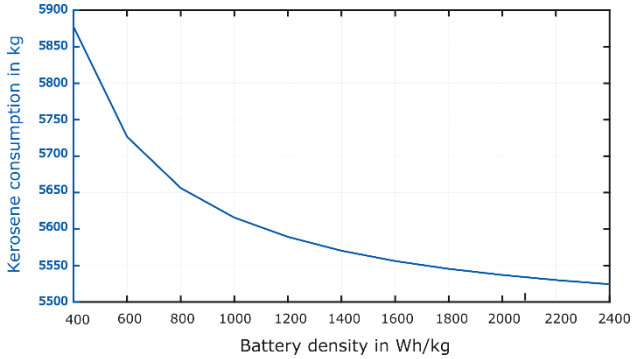

BILD 10 Sensitivity towards battery energy density

BILD 10 shows the total energy consumption and the battery mass plotted against the battery energy density of eRay with 200 PAX and a 6000km range. Even if available, batteries with ultra-high energy densities of 2500 kWh/kg or higher achieve a maximum total energy cut of only 2 percentage points compared to eRay's 1400 kWh/kg.

4.3.4. Electrical Components

To reach the goal of high overall energy efficiency of the airplane, an efficient powertrain concept is essential for distributing energy from the gas turbines to the EFANs. Multiple components are needed for the turboelectric propulsion system. The electrical system architecture described in this report can be seen in BILD 15 found in the Appendix. A generator is attached to a turbine engine that is sitting on the wing tip producing electric energy to power the distributed EFANs. The battery, which is located in the belly of the aircraft, is the second available source of energy. The battery feeds into the power system during taxi, take-off and climb. In flight, it is charged by the turbine and the generator. Batteries require DC current [49]. The generator next to the engine produces AC current. DC systems have some overall advantages considering cable diameters and electromagnetic tolerance [50]. On the other hand, AC motors tend to be better suited for large scale high power-density applications [24]. Engine speed correlates directly to the current frequency. Using inverters is a requirement for an overall DC system. Each EFAN is powered by an AC motor and can be controlled individually.

The key factors for optimizing the electrical propulsion system are high power densities and high efficiencies of the components. Conventional motors, generators and inverters can be used, like the "1MW High Efficiency Generator" concept, which was introduced and advertised by the company Honeywell in 2015 and predicts a power density of 8kW/kg for an oil conduction and spray cooled generator. Remarkable is the estimated efficiency of 0.98 compared to current generators running at an efficiency below 0.9 [51]. The propulsion system of the baseline is based on conventional components like the Honeywell generator and is estimated to have an overall efficiency of 85% as technology is advancing. An extremely promising approach to further reducing the weight of the electric propulsion system are current developments in the field of cryogenically cooled superconducting components. Providing a suitable heat sink for superconducting elements within the electrical system may lead to better power densities for generators, motors and inverters as superconducting materials do not have any remarkable electrical resistance below a certain temperature [37]. This enables a high current to run through only small diameter wires, reduces resistance related dissipation of energy at the motor and promises "light, compact, very efficient motors and generators" [37]. A study by the Royal Aeronautical Society in London mentions the possibility to reduce the weight of the components by half when using superconducting materials [52]. This is backed by a Bauhaus Luftfahrt study predicting power densities of motors and generators to improve from 10 kW/kg to 20kW/kg until 2035 [53] - which is more than twice the predicted power density of the Honeywell 1MW High Efficiency Generator [51]. The AC motors of the EFANs require inverters like the ones based on Solid State Power Converters (SSPCs). These inverters are currently operating at an efficiency of 95% and a power density of 10 kW/kg [53, 54]. A NASA contract project predicts power densities of 25kW/kg compared to the 10kW/kg at the moment and efficiencies of 99.5% for combined inverter and cryocooler systems [54].

The potential of superconducting components is undisputed. The big challenge lies within supplying the necessary heat sinks to reach the temperatures mentioned above required by the superconducting materials. This may be achieved in different ways: Either by using liquid hydrogen (that could also be used to fuel the aircraft) or by using a refrigerator system with a coolant like nitrogen [37]. The aircraft design described in this report does not include hydrogen but conventional jet fuel. Carrying an extra hydrogen fuel tank increases the complexity of the aircraft and leads to further difficulties like hydrogen embrittlement as described in [55]. The design introduced in this report focuses on refrigerator systems. These systems inherit a complex trade-off: while enabling the use of superconducting HT components, which leads to high power densities and efficiencies, they also increase the complexity and weight of the aircraft design which might annul the advantages. The technological development of refrigerator systems in the next 20 years is extremely uncertain [37]. Due to the high uncertainty of the development of refrigerator systems and the possible difficulties regarding weight and complexity of the cryocooler, the baseline concept was calculated with parameters of conventional electric components. The eRay is more optimistic about these developments and has a refrigerator system using nitrogen to profit from the high efficiencies and great power densities of superconductors.

4.4. Control and Stability

The baseline concept is equipped with conventional empennage and control surfaces in an aerodynamic stable configuration. To enhance energy efficiency, the eRay is designed for neutral lateral-directional and longitudinal static stability. Consequently, fly by wire with a control system to avoid uncontrolled flying conditions is implemented. Additionally, the rudder is replaced by thrust variation of EFANs for directional control. As requirements for directional stability are lowered, the horizontal tail is implemented with dihedral angle Γ for neutral directional stability. Consequently, no vertical tail is assembled. This feature does not meet regulation CFR Part 25, however, the FAA issued a special condition for the Airbus A350, allowing it to operate in neutral state, if special requirements are met [56]. The estimation of dimensions of control surfaces and the thrust that must be provided for control is described in following part and is derived from Raymer [21]: First, the horizontal tail area is determined to meet neutral stability criterion $C_{M\alpha} = -C_{L\alpha}(\bar{X}_{np} - \bar{X}_{cg}) = 0$. Here, $C_{M\alpha}$ is the pitching moment with respect to the angle of attack, $C_{L\alpha}$ is $\frac{dC_L}{d\alpha}$, $\bar{X}_{np}$ / $\bar{X}_{cg}$ is the distance from nose to neutral point/center of gravity.

After determining the dihedral angle of the tail for directional stability, it is resized according to $S_{h,re} = \frac{1}{\cos\Gamma} S_h$ to 29.7m² [57]. For directional static stability, $\frac{\Delta T \overline{Y_p}}{qS_w}$ for thrust variation is added and the term for the vertical tail is replaced by one for the horizontal tail with a dihedral angle:

(3) $C_n = C_{n\beta_w}\beta + C_{n\delta_a}\delta a + C_{n\beta fus}\beta + \sin(\Gamma)C_{n\beta h}\beta + \frac{\Delta T \overline{Y_p}}{qS_w}$ *

$C_{n\beta h}$ can be taken from horizontal tail calculation. To meet the requirement of neutral directional stability, $\frac{\delta C_n}{\delta \beta} = 0$, cruise is investigated, being the most critical condition due to a small stabilizing effect of the wing. With eq. (3), the minimum required dihedral angle is given with 19.9° for a horizontal tail area of 27.9m².

The roll moment in coefficient form is given in eq. (4):

(4) $C_l = C_{l\beta w} \cdot \beta + C_{l\delta a}\delta_a + \sin(\Gamma)C_{l\beta h} \cdot \beta$

The coefficients in eq. (4) are calculated for given geometry and aileron placement using empirical formulas. $C_{l\beta w} \cdot \beta$ / $\sin(\Gamma)C_{l\beta h} \cdot \beta$ is the roll moment of the wing/dihedral horizontal tail due to slip, $C_{l\delta a}\delta_a$ due to aileron deflection. Longitudinal stability is present if $\frac{\delta C_l}{\delta \beta} = C_{l\beta\omega} + \sin(\Gamma)C_{l\beta h} < 0$.

This condition is given because both terms of the sum are negative, as the wing has positive sweep and the horizontal tail has an upward dihedral. Situations of concern for stability are one sided thrust collapse and crosswind landings [21]. First issue is of no concern due to multiple redundancy of 21 EFANs. However, crosswind landings must be considered. Crosswind landings equal a sideslip with β = 11.5°, that results in coupled yaw and roll moment. The roll moment is counteracted by ailerons, the yaw moment by thrust variation. The aileron deflection is set to 20°, resulting in aileron dimensions and placement shown in BILD 16 Appendix. Thrust variation is calculated using eq. (3). C_n must be zero for stationary flight, resulting in $\frac{\Delta T \bar{Y}_p}{qS_\omega} = 0.0305$ or $\Delta T = 30.8\text{kN}$ respectively. The ΔT is achieved by increasing thrust by 15.4kN on the side exposed to the approaching flow and reducing it by 15.4kN on the other side, keeping total thrust constant. This is done automatically by the control system.

*[C_n is the yaw-moment coefficient, $C_{n\beta}$ is the yaw-moment coefficient in respect to the yaw angle β. W refers to wing, fus to fuselage, h to horizontal tail. The product $C_{n\delta_a}\delta a$ gives the yawing moment due to aileron deflection. ΔT is the thrust difference of right wing fans to left wing fans, $\overline{Y_p}$ is the normalized average distance from right wing fans to left wing fans. S_w is the wing area and q the dynamic pressure.]

4.5. Energy Consumption

Using the masses and efficiency coefficients calculated in section 4, the energy consumption per segment is calculated in table 3. The mission is set according to BILD12 for a distance of 4200km and maximum payload. In all cases, cruise contributes the major part with approximately 85% of overall energy consumption. During descent, in both developed concepts the energy consumption is marginal as the EFANs are shut off. Note, that the given values represent the needed energy per segment, and that this is decoupled from the core turbine as a battery as buffer is used. In descent, the gas turbines produce electric power even though power consumption is almost zero.

	A321	Baseline	eRay
Takeoff	2.94	1.62	1.28
Climb	7.35	5.22	4.51
Cruise	71.91	46.07	33.78
Descent	2.27	0.01	0.01
Mission	84.47	52.92	39.57
Kerosene fuel in kg	15881	8055	5782
Kerosene/PAX/100km in l	2.36	1.14	0.82
Improvement	/	51.7%	65.3%

TAB 3 Energy Consumption per Segment in MWh

4.6. Cabin Concept

Today, the first concept of virtual windows is entering service within the new First Class in Emirates' Boeing 777-300ER [58, 59]. By 2045, eRay's windowless cabins will have gained wide acceptance by passengers. The window mock ups in the cabin are underlaid with high definition Organic Light Emitting Diodes (OLED) Displays to create a feeling comparable to a fuselage with windows [60]. The EASA CS-25 requirements concerning minimum aisle width and for three 'type A' and two 'type I' emergency exits per side for more than 200 PAX are met and shown in BILD 11 [61]. Guaranteeing safe evacuation during an emergency requires an outside view for the crew as each emergency exit "must have means to permit viewing of the conditions outside the exit when the exit is closed" according to Part 25 of FAA regulations [61]. Therefore, the doors and

emergency exits will provide windows to ensure undisturbed vision for evacuation [61]. Independent of the seating configuration, the belly is able to store a total of ten LD-3 45W containers. eRay is offered with different seating options, three of them are shown:

- Single Class with Economy Seats: 200 seats are placed in a 3-3 conventional layout. The legroom distance and the passenger area are comparable to today's Airbus A321 layout.
- High density configuration: Premium Economy, Economy Slim. The ultra-high-density configuration can transport 222 PAX using Economy seats as well as Economy Slim seats for a 3000km range configuration. The Economy Slim seats offer a more upright seating experience for the passengers to reduce seat spacing and make use of the dead volume above the heads of the passengers. Economy Slim reduces the distance between rows to approximately 80% of the regular seats [62, 63, 64]. Fitting these seats with the height of 153cm requires a slight shift of the aisle off center, see BILD11. On the Economy Slim side of the aisle, the storage volume for carry-on luggage is not reduced compared to Economy, but even increased by more than 30%, paying attention towards the importance of hand luggage for passengers. The EASA CS-25 requirements concerning minimum aisle width and for three type A and two type I emergency exits per side for more than 200 PAX are met.
- Three Class Configuration: Business, Premium Economy, Economy Slim. The three-class configuration features a traditional layout for a medium range aircraft. It has eight Business class, 87 Economy and 105 Economy Slim seats.

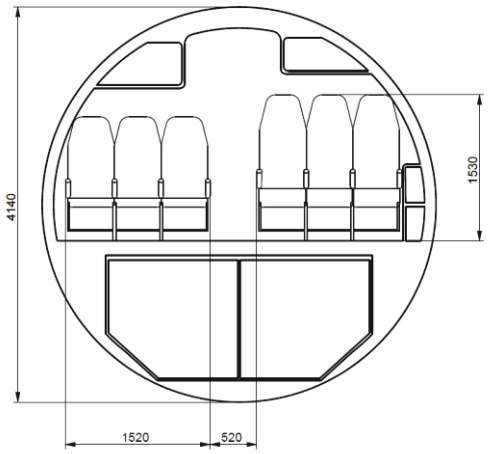

BILD 11 High Density Cabin Layout - Side View

4.7. Summary Baseline and eRay Concept

With the previously described measurements, the energy consumption of the eRay was reduced drastically by simultaneously improving the mission profile compared to the payload range diagram of an A321 (see BILD12).

TAB 4 provides an overview of the most relevant aspects differentiating the baseline and the more optimistic eRay concept. Also, the resulting savings in mass reduction, (L/D) ratio and the overall efficiency of the propulsion system are shown.

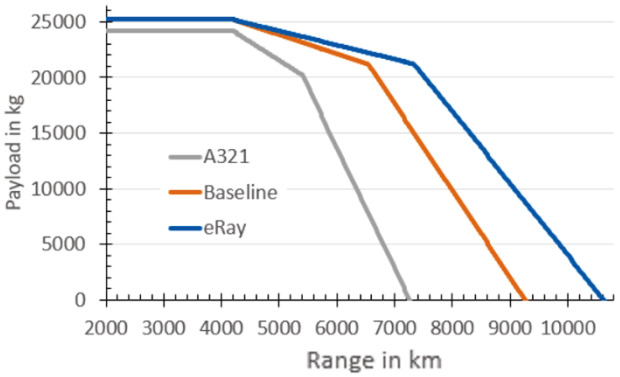

BILD 12 Payload Range Diagram for A321, Baseline and eRay

These results show the big potential of both, the baseline eRay concept in a rather pessimistic scenario concerning the development of certain key technologies described in section 6.1 as well as the more optimistic eRay variant which offers even higher savings. The following sections use the best case eRay concept as a reference for further considerations like the concept of operations (see section 5) and the comparison to the current best in class reference aircraft Airbus A321.

	Baseline	eRay
Mass reduction (empty)	16%	28%
(L/D) improvement	23%	28%
Span	36m	38m
η_{ov} improvement	25%	50%
Battery density	800 Wh/kg	1400 Wh/kg
Regulations applied	CS-25	Modified CS-25
Turbine efficiency	0.56	0.57
Windows	Standard Configuration	No passenger windows except for emergency exits
Cockpit Design	Cockpit with pilot assistance systems	Single pilot cockpit
Lateral stability and control	Conventional tail and stable	Neutral stable and no vertical tail
Ultimate load wing	3.3	2.7
Electric propulsion system	Efficiency 0.85, conventional components	Efficiency 0.98, superconducting components

TAB 4 Baseline and eRay Design

5. OPERATION CONCEPT

A Concept of Operations (CONOPS) describes a proposed system from the user centered viewpoint of multiple stakeholders. It is meant to demonstrate and communicate system characteristics in an easily understandable way to everyone involved [66]. The overall purpose of the eRay is to enable transport that is safe, cheap and environmentally friendly. Operating an aircraft is a very complex process.

Several different stakeholders profit from the eRay's advantages over different phases of flight.

Scheduling and routing: Not many airport related constraints are relevant when planning the routing and schedule of an eRay fleet. Only the batteries are used for taxi, take-off and landing leading to neither emissions nor noise regulations being a critical factor for routing. The eRay may operate at airports with night bans if regulations are changed regarding its way of operating silently and pollution free. Thus, new slots can be offered extending the limited airport capacities. eRay excels the ETOPS 180 criteria, enabling unlimited operations in its key market Asia Pacific and even traversing the Atlantic Ocean on a 6000km mission making it an attractive choice for European as well as North American carriers.

Ground handling: The eRay recharges its batteries in flight so no charging infrastructure or battery changing is required during ground handling. The wing span of 38m fits the standard ICAO airport bays using its highly maneuverable landing gear to park oblique in the standard 36m x 36m bay. Deicing trucks are upgraded for cleaning off dusts and mosquitoes of the laminar wings every fifth landing, ensuring pure wing surfaces and highly efficient laminar flow during cruise.

In flight (Take-Off, Climb, Cruise, Descent, Landing): Boarding is simple and efficient due to eRay's cabin layout. Passengers are provided with an outside view through HD displays integrated into the cabin walls. A voice assistant based on artificial intelligence allows passengers to communicate with the cabin crew and transmit personal preferences like individual temperature sensitiveness and food choices. An innovative lighting concept using natural light helps passengers to overcome jet lag. It creates a soothing atmosphere meeting the demands of people with fear of flying. It is used for guidance during emergency evacuation and may also include airline's corporate identity design features. Emergency evacuation happens through exits meeting current CS-25 requirements as stated in section 4.6. Further Human Machine Interface developments were able to overcome the ironies of automation [67] and reduce the pilot's workload without affecting situation awareness negatively [68]. The cockpit requires only one pilot as redundancy for monitoring purposes due to the extremely low probability of failure of the autopilot and for aid in an emergency situation [69].

6. FEASIBILITY: KEY TECHNOLOGIES

In this section, key technologies for this concept are summarized and evaluated according to Technology Readiness Level (TRL) [70]. Furthermore, the sensitivity of eRay regarding each technology is shown through the increase of consumption if not implemented. The neutral configuration is already common in state of the art aircraft as the Airbus A350-900, only yaw-control through engines is not implemented yet. However, the control technology of recent UAV proof the feasibility of this concept. The readiness of LFC is e.g. shown by the Boeing 757 HLFC test flight in 1990 [32]. Engine intercooling was successfully tested on a rig at Chalmers University, Gothenburg, Sweden [71]. Recuperators are tested on a small scale in laboratories as well [72, 73]. Turbines with recuperator have been used in micro turbines on ground applications as in the tank M1A1 Abrams or for energy production [39].

	TRL	Energy-Sensitivity
Laminar Flow Control	7	28.2%
Neutral config. w/o rudder	6	6.5%
Refrigerator	4	13.7%
IRA Engine	4-5	12.2%
High Density Battery	3	1.7%
Single-Pilot Cockpit	6	/
Active load reduction	6	1.8%

TAB 5 Key Technologies, TRL and Energy-Sensitivity for eRay

7. CONCLUSION

The ambitious requirements to decrease energy consumption by at least 60% on top of other characteristics described in section 1 are fully satisfied by eRay. Using the synergy effects of TEDP, eRay combines the advantages of using LFC and the minimum noise potential of battery powered flight close to airports while offering a large degree of system safety. The propulsive fuselage draws full profit from BLI at the aft of the fuselage, leading to even more power savings. A conventional body-wing layout increases compatibility with existing airport infrastructure. Even the conservative baseline concept calculated with a modest estimation of parameters and design changes turns out to be 25% better in overall efficiency of propulsion compared to the A321. The Best Case eRay variant based on a more optimistic estimation of parameters and design features takes the design one step further to show the new aircraft's full potential. An overall propulsion efficiency improvement of 50% is possible, along with mass reduction of 28% and an (L/D) improvement of 28%. The Payload Range Diagram in BILD 12 shows that eRay outperforms the A321 by far. With 20t payload, 7850km can be flown instead of 5400km with the A321, making eRay an attractive midrange aircraft. eRay is well suited for everyday operations. Ground handling is easy as no noteworthy effort is needed compared to the A321. Furthermore, a successful product is also described through the look and feel perceived by the customer. eRay's cabin layout satisfies the demands of price sensitive passengers booking standing seats in Economy Slim and captivates customers with a modern and functional feel-good atmosphere. Overall, the eRay Aircraft Concept can in fact be seen as a solution for the challenges of the future, flying efficient, silent and just as elegant as the electric ray that strides through the sea.

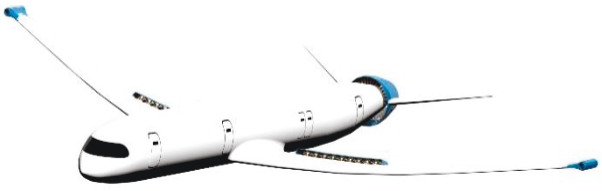

APPENDIX

SKRIPTUM

[1] David Oxley. Air Passenger Market Analysis December 2017. IATA. 2017.
[2] Robert B. Jackson et al. “The Environmental Costs and Benefits of Fracking”. In: Annual Review of Environment and Resources (2014)
[3] Flightpath 2050: Europe’s vision for aviation; maintaining global leadership and serving society’s needs; report of the High-Level Group on Aviation Research. Policy / European Commission. Publ. Off. of the Europ. Union, 2011.
[4] National Aeronautics and Space Administration. Green Aviation: Safeguarding Our Future on Earth Fact Sheet. 2015
[5] World urbanization prospects, the 2014 revision: Highlights. New York: United Nations, 2014.
[6] United Nations. World Population Prospect 2017 - Key findings & advanced tables. 2017.
[7] OAG.Key facts behind the world’s 20 busiest routes: Based on frequency in the 12 mounts to February 2018. 2018.
[8] Airbus SE.Global Market Forecast: Growing Horizons 2017 / 2036. 2017.
[9] M. M. Haines et al. “Chronic aircraft noise exposure, stress responses, mental health and cognitive performance in school children”. In: Psychological Medicine (2001)
[10] Flughafen Zürich. Lärmgebühren: Lärmgebühren für Strahlflugzeuge. Zürich, Schweiz, 2013.
[11] Swedavia Airports. Airport Charges: Airport Charges for Swedavia AB. 2016.
[12] Amsterdam Airport Schiphol. Airport charges and conditions 2017: Summary. 2017
[13] Süddeutsche.de GmbH, Munich, and Germany. Ein fatales Signal für München. 2018. url: http://www.sueddeutsche.de/muenchen/flughafen-ausbau-ein-fatales-signal-fuer-muenchen-1.3869169 (visited on 06/16/2018).
[14] Taylor, Matthew. Government faces growing pressure over Heathrow third runway. Ed.by TheGuardian.com. 2018. url:https://www.theguardian.com/environment/2018/jun/15/government-faces-growing-pressure-over-heathrow-third-runway (visited on 06/15/2018).
[15] EuroControl. Challenges of Growth 2013: Summary Report. 2013
[16] FlightView. Convenience & Choice: What Travelers Want Most (And Are Willing to Pay For) Throughout Their Journey: How Airlines and Airports Can Capture More Revenue & Loyalty by Improving the Travel Experience. 2015
[17] Scott McCartney. The Rare Case Where Airlines and Passengers Both Win. The Wall-street Journal. 2018. url: https://www.wsj.com/articles/the-rare-case-where-airlines-and-passengers-both-win-1522246644 (visited on 06/19/2018).
[18] Morphet, H. and Bottini, C.Air connectivity: Why it matters and how to support growth. 2014. (Visited on 06/19/2018).
[19] Airbus SE. A321 Aircraft Characteristics: Airport and Maintenance Planning. 2018
[20] Egbert Torenbeek. Synthesis of subsonic airplane design: An introduction to the preliminary design of subsonic general aviation and transport aircraft, with emphasis on layout, aerodynamic design, propulsion and performance. 1996
[21] Daniel P. Raymer. Aircraft Design. 4th ed. AIAA education series. American Inst. Of Aeronautics and Astronautics, 2006
[22] Joachim Scheiderer. Angewandte Flugleistung: Eine Einführung in die operationelle Flugleistung vom Start bis zur Landung. Berlin, Heidelberg: Springer-Verlag Berlin Heidelberg, 2008
[23] Harshad Khadilkar and Hamsa Balakrishnan. “Estimation of Aircraft Taxi-out Fuel Burn using Flight Data Recorder Archives”. In: AIAA Guidance, Navigation and Control Conference. [American Institute of Aeronautics and Astronautics], 2011
[24] Seitz A. and Schmitz O. Electrically Powered Propulsion: Comparison and Contrast to Gas Turbines. (Visited on 05/26/2018)
[25] R. Wittmann. Passenger Acceptance of BWB Configurations
[26] Hans-Jörg Steiner. Multi-Disciplinary Design and Feasibility study of Distributed Propulsion Systems. 2012
[27] Gregorio Ameyugo, Mark Taylor, and Riti Singh. “Distributed Propulsion Feasibility Studies”. In:25th International Congress of the Aeronautical Science (2006)
[28] Hyun Dae Kim, Gerald V. Brown, and James L. Felder. Distributed Turboelectric Propulsion for Hybrid Wing Body Aircraft. 2008
[29] Jan Roskam. Airplane design. DARcorporation, 2002
[30] I. Salah El Din et al. “Natural Laminar Flow Transonic Wing Design Applied to Future Innovative Green Regional Aircraft”. In:3AF/CEAS Conference” Greener Aviation: Clean Sky breakthroughs and worldwide status” (2014)
[31] M. Nit ̧a and D. Scholz. “Estimating The Oswald Factor From Basic Aircraft Geometrical Parameters”. In: Deutscher Luft- und Raumfahrtkongress (2012)
[32] Ronald Joslin. Overview of Laminar Flow Control. 1998
[33] T. Takahashi et al. “Zero Lift Drag and Drag Divergence Prediction for Finite Wings in Aircraft Design”. In:48th AIAA Aerospace Sciences Meeting Including the New Horizons Forum and Aerospace Exposition (2010)
[34] J. J. Thibert, J. Reneaux, and V. Schmitt. “Onera Activities On Drag Reduction”. In:Office National d’Etudes et de Recherches Aèrospatiales(1999)
[35] M.A.B. van den Berg. “Internal Systems Design for Smart Fixed Wing Technologies using Knowledge Based Engineering”. 2010
[36] R.D. Joslin. “Aircraft Laminar Flow Control”. In: Annual Review of Fluid Mechanics (1998).
[37] Hyun Dae Kim. Distributed Propulsion Vehicles. 2010.
[38] Williams, Butler, and Wood. “The Aerodynamics of Jet Flaps”. In: Aeronautical Research Council - Reports and Memoranda (1961)
[39] Willy J. G. Bräunling. Flugzeugtriebwerke: Grundlagen, Aero-Thermodynamik, ideale und reale Kreisprozesse, thermische Turbomaschinen, Komponenten, Emissionen und Systeme. 4. Aufl. VDI-Buch. Berlin: Springer Vieweg, 2015
[40] Seitz, A. and Gologan, C. “Parametric design studies for propulsive fuselage aircraft concepts”. In: CEAS Aeronautical Journal (2015)
[41] Joerg Sieber. Overview New Aircraft Engine Core Concepts. MTU. 2009
[42] G. Wilfer et al. “New Environmental Friendly Aero Engine Core Engines”. In: 18th International Symposium on Air Breathing Engines (2007)

[43] Aeronautics and Space Engineering Board - National Research Council. Aeronautical technologies for the twenty-first century. 1992. url: http://search.ebscohost.com/login.aspx?direct=true&scope=site&db=nlebk&db=nlabk&AN=731
[44] Joerg Henne. Technologie & Entwicklung von Triebwerken der nächsten Generation. MTU.2017
[45] M. R. Reyhani et al. “Turbine blade temperature calculation and life estimation – a sensitivity analysis”. In: Propulsion and Power Research (2013)
[46] Yuan Yang et al. “New nanostructured Li2S/silicon rechargeable battery with high specific energy”. In: Nano letters (2010). (Visited on 06/03/2018)
[47] Süddeutsche.de GmbH, Munich, and Germany.Bosch gibt Forschung zu neuen Batteriezellen auf. 2018. url: http:/www.sueddeutsche.de/wirtschaft/e-autos-bosch-gibt-forschung-zu-neuen-batteriezellen-auf-1.3886227 (visited on 06/19/2018)
[48] G. Girishkumar et al. “Lithium−Air Battery: Promise and Challenges”. In: The Journal of Physical Chemistry Letters(2010)
[49] Thomas Reddy. Linden’s Handbook of Batteries, 4th Edition. New York: McGraw-Hill, 2010
[50] M. Becherif and M. Y. Ayad. “Advantages of variable DC bus voltage for Hybrid Electrical vehicle”. In:2010 IEEE Vehicle Power and Propulsion Conference.
[51] Cristian Anghel. Hybrid Electric Propulsion Technologies - 1MW High Efficiency Generator. url: http://www.nianet.org/ODM/presentations/CristianAnghel-Honeywell-HoneywellTechnologiesforHybridElectric Propulsion(002).pdf.
[52] Greener by Design Science and Technology Sub Group London. “Air Travel–Greener by Design Mitigating the environmental impact of aviation: Opportunities and priorities”. In: The Aeronautical Journal (2005).
[53] H. Kuhn et al. “Progress and Perspectives of Electric Air Transport”. In: Proceedings of the 28th International Congress of the Aeronautical Sciences. Bauhaus Luftfahrt e.V.,2012
[54] G.V. Brown. “Weights and Efficiencies of Electric Components of a Turboelectric Aircraft Propulsion System”. In: AIAA 2011-225, 49th AIAA Aerospace Sciences Meeting including the New Horizons Forum and Aerospace Exposition, 4-7 January, Orlando, Florida, 2011
[55] Afrooz Barnoush. Hydrogen embrittlement, 2008
[56] Federal Aviation Administration. Special Conditions: Airbus Model A350-900 Series Airplane; Electronic Flight-Control System: Lateral-Directional and Longitudinal Stability, and Low-Energy Awareness. 2014. url: https://www.federalregister.gov/documents/2014/07/25/2014-17575/special-conditions-airbus-model-a350-900-series-airplane-electronic-flight-control-system (visited on 06/26/2018).
[57] E. Purser and O. Campbell Experimental Verification of a simplified Vee-Tail Theory and Analysis of available data on complete models with Vee Tails: NACA 823. 1945.
[58] Emirates. Emirates Boeing 777 Game Changer: Enjoy HD views. 2018. url: https://www.emirates.com/english/experience/our-fleet/boeing-777/gamechanger/ (visited on 06/17/2018)
[59] Whitehead, Johanna. Emirates Airline introduces virtual windows for first class passengers. Ed. by The Independent. 2018. url: https://www.independent.co.uk/travel/news-and-advice/emirates-airline-virtual-windows-first-class-passengers-fuel-costs-a8393266.html (visited on 06/17/2018)
[60] S. Bagassi, F. Lucchi, and F. Persiani. “Aircraft Preliminary Design: A windowless concept”. In: 5th CEAS Air & Space Conference. University of Bologna. 2015
[61] Federal Aviation Administration. Federal Aviation Regulations (FAR) Part 25-Airworthiness Standards: Transport Category Airplanes.url: https://www.ecfr.gov/cgi-bin/text-idx?node=14:1.0.1.3.11#se14.1.251103
[62] AvioInteriors. Aviointeriors Skyrider 2.0-Aviointeriors. 2018. url: http://aviointeriors.it/2018/press/aviointeriors-skyrider-2-0/ (visited on 06/28/2018)
[63] Tamara Hardingham-Gill and CNN. Will new stand-up airplane seat take off? 2018. url: https://edition.cnn.com/travel/article/standing-up-airplane-seat/index.html (visited on 05/27/2018)
[64] Dan Milmo. Ryanair plan for standing-only plane tickets foiled by regulator. Ed. by The Guardian. 2012.url: https://www.theguardian.com/business/2012/feb/28/ryanair-standing-only-plane-tickets-regulator (visited on 06/28/2018)
[65] Cord-Christian Rossow, Martin Hepperle, and Heiko Frhr. von Geyr. The 1g-Wing, Visionary Concept or Naive Illusion. Bericht des Instituts für Aerodynamik und Strömungstechnik, DLR. 2016
[66] IEEE-Institute of Electrical and Electronics Engineers. IEEE Guide for Information Technology-System Definition-Concept of Operations (ConOps). 1998
[67] Lisanne Bainbridge. “Ironies of automation”. In: Automatica (Nov. 1983)
[68] D. Comerfeld and et al. NASA’s Single-Pilot Operations Technical Interchange Meeting: Proceedings and Findings. NASA. 2013
[69] Joel Lachter et al. Towards Single Pilot Operations: Developing a Ground Station. NASA. 2014
[70] NASA. Technology Readiness Level Definition. url:https://www.nasa.gov/pdf/458490mainTRLDefinitions.pdf (visited on 06/27/2018)
[71] Xin Zhao. Aero Engine Intercooling: Conceptual design and experimental validation of an aero engine intercooler. 2016
[72] Mario L. Ferrari et al. Recuperator dynamic performance: Experimental investigation with a microgas turbine test rig. 2011
[73] Kyu Hyung Do et al. Experimental investigation on the pressure drop and heat transfer characteristics of a recuperator with offset strip fins for a micro gas turbine. 2016
[74] Airbus SE. Airbus Aircraft 2018 Average List Prices. 2018
[75] K. Willcox. Aircraft Systems Engineering Costs Analysis: Aerospace Computational Design Laboratory, Massachusetts Institute of Technology. 2004
[76] J. P. Hampstead. Has Tesla hit a wall on battery cost improvements? 2018 url: https://www.freightwaves.com/news/2018/2/28/has-tesla-hit-a-wall-on-battery-cost-improvements (visited on 06/26/2018)
[77] RWTH Aachen. CeRAS-Central Reference Aircraft Data System. 2018. url: http://ceras.ilr.rwth-aachen.de/ (visited on 06/03/2018)
[78] Johanning A. and Scholz D. Evaluation of Worldwide Noise and Pollutant Emission Costs for Integration into Direct Operating Cost Methods. 2012
[79] IATA.IATA-Jet Fuel Price Monitor. 2018. url: http://www.iata.org/publications/economics/fuel-monitor/Pages/index.aspx (visited on 06/26/2018)

FURTHER FIGURES

	Weigth	Prop-Efficiency	Transmission Efficicency	Complexity	Noise	Passenger Acceptance	Synergy Effects	Development Risk	Safety	
Geared TurboFan	-1	1	0	-1	1	0	0	0	0	
Open-Rotor	-1	2	0	-2	-1	-2	0	-1	-1	
Electric Propulsion	-3	3	-1	-2	3	-1	3	-3	2	
Turbo-Electric Propulsion	-2	3	-3	-3	2	0	3	-1	3	
Weighting:	3	5	3	2	3	3	3	2	5	29
Normalized weights:	0,10	0,17	0,10	0,07	0,10	0,10	0,10	0,07	0,17	

	Weigth	Prop-Efficiency	Transmission Efficicency	Complexity	Noise	Passenger Acceptance	Synergy Effects	Development Risk	Safety	Score
Geared TurboFan	-0,10	0,17	0,00	-0,07	0,10	0,00	0,00	0,00	0,00	0,10
Open-Rotor	-0,10	0,34	0,00	-0,14	-0,10	-0,21	0,00	-0,07	-0,17	-0,45
Electric Propulsion	-0,31	0,52	-0,10	-0,14	0,31	-0,10	0,31	-0,21	0,34	0,62
Turbo-Electric Propulsion	-0,21	0,52	-0,31	-0,21	0,21	0,00	0,31	-0,07	0,52	0,76

BILD 13 Appendix: Exemplary Decision Table for qualitative Selection

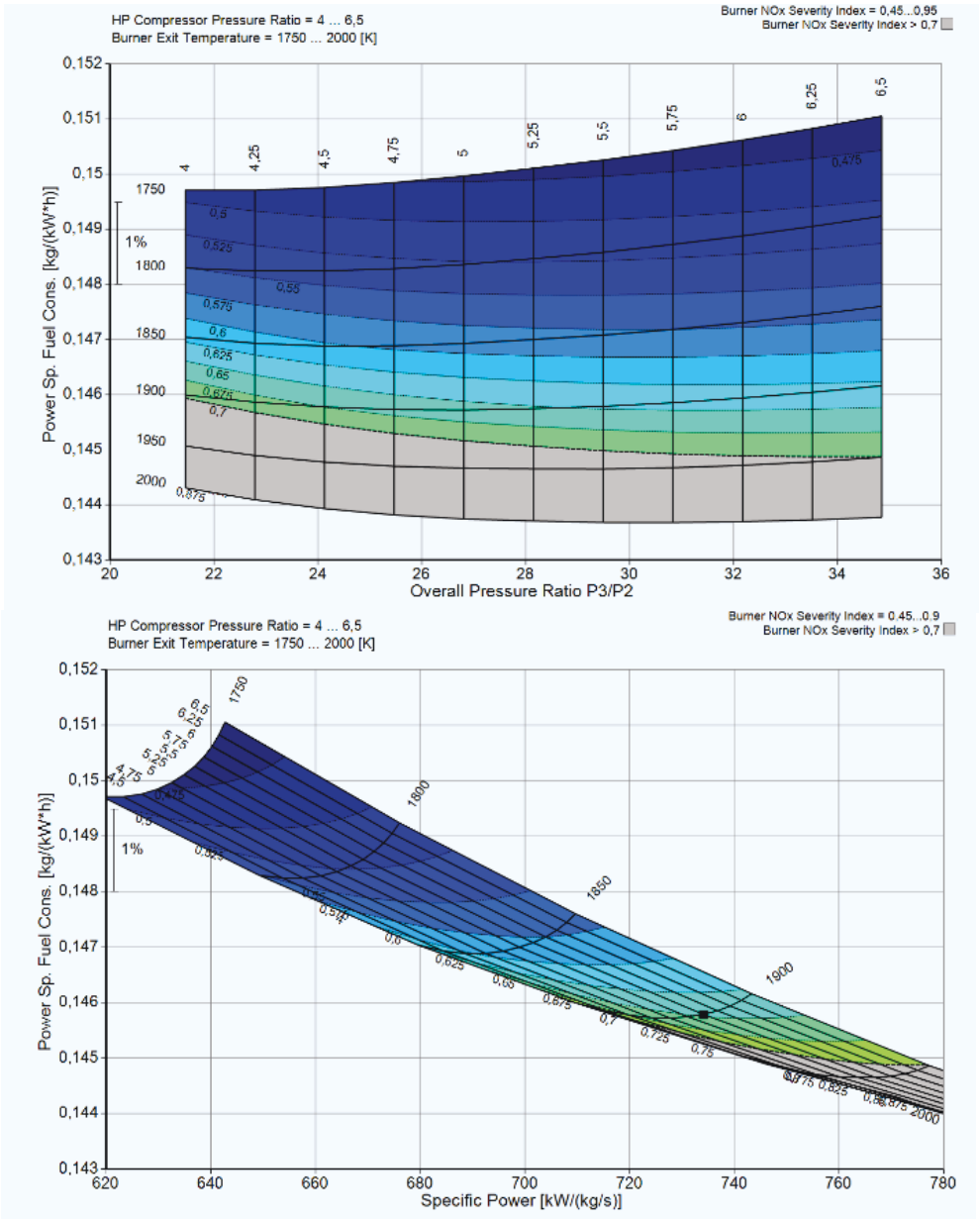

BILD 14 Appendix: (a) PSCF vs OPR, (b) PSCF vs SP

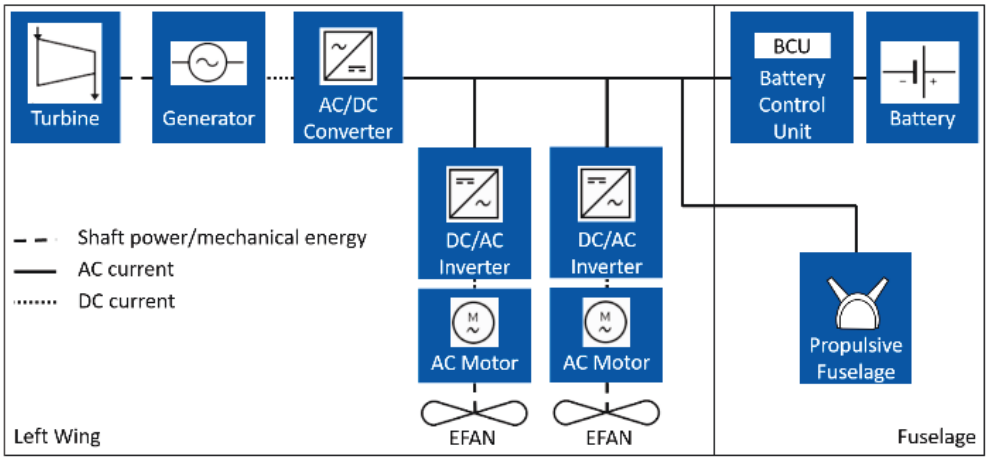

BILD 15: Appendix: Electric Propulsion System - Schematic arrangement, not to scale

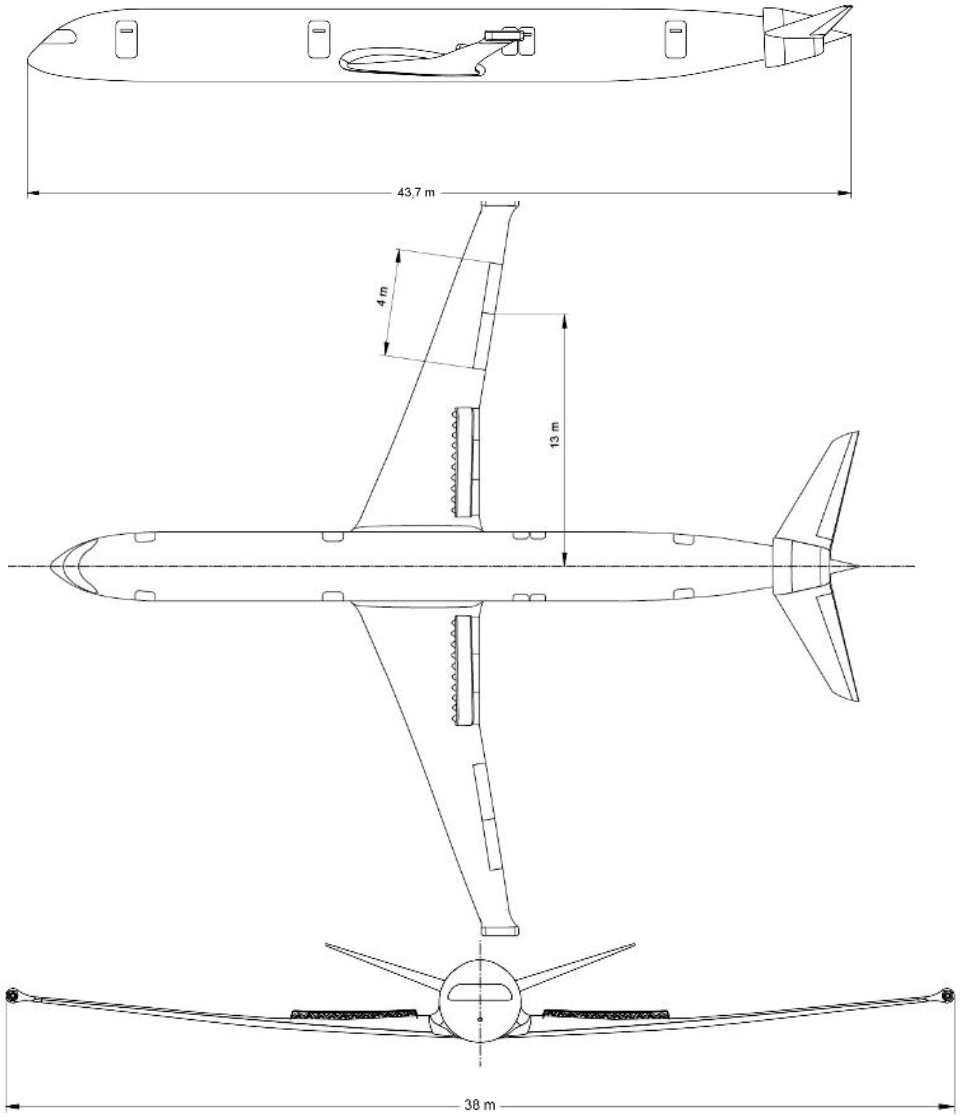

BILD 16: Appendix: 3 sides views